International Journal of Innovative Technology and Interdisciplinary Sciences
www.IJITIS.org
ISSN:2613-7305
Volume 5, Issue 3, pp. 942-953, 2022
DOI: https://doi.org/10.15157/IJITIS.2022.5.3.942-953
Received February 11, 2022; Accepted April 18, 2022

Calculation and Simulation of Vehicle Steering Dynamics

Vu Trieu Minh[*a1], Reza Moezzi[b2], Klodian Dhoska[c3]

[1]School of Engineering, Tallinn University of Technology, Tallinn, Estonia

[2]Institute for Nanomaterials, Advanced Technologies and Innovation, Technical University of Liberec, Czech Republic

[3]Department of Production and Management, Faculty of Mechanical Engineering, Polytechnic University of Tirana, Albania

*[a]vutrieuminh@gmail.com; [b]rezamoezy@gmail.com; [c]kdhoska@upt.al

ABSTRACT

This paper presents fundamental mathematical estimations of vehicle sideslip in stationary conditions regarding the influences of the vehicle parameters such as the tire stiffness, position of gravity centre, vehicle speed and the turning radius. The vehicle dynamics on steady state and transient responses are also investigated to see the effects of the yaw natural frequency and yaw damping rate on the steering system. Results from this study can be used in designing an automatic control of tracking vehicle in the future.

Keywords: Sideslip angle, yaw damping rate, steady state response, transient response.

1. INTRODUCTION

Calculation and simulation of vehicle steering dynamic are essential for any control systems since most of the modern vehicles are currently equipped with new electronic stability and auto-guided systems. The accurate determination of the sideslip angle can help to improve the yaw and the steering stability performance. Sideslip estimation is based on the vehicle physical variables (mass, gravity position, tire stiffness), vehicle speed, lateral acceleration, steering angle, and yaw rate. Unlike yaw rate, the vehicle sideslip angle cannot be measured directly; hence estimation methods have been developed to calculate the sideslip angle from the available above variables.

Among the latest research papers on this issue, in [1] it has been proposed a sideslip angle estimation method that considers severe longitudinal velocity variation over the short period of time based on extended Kalman filter (EKF). At [2] it has been established an estimation method of vehicle roll angle, lateral velocity and sideslip angle. Only roll rate sensor and the sensors readily in electronic stability control (ESC) are used in this estimation process. Mathematical algorithms are based on kinematic relationships, and then, avoiding dependence on vehicle and tire models, which can minimize tuning efforts and sensitivity to parameter variations. In the research work at [3] it has been introduced an observer for dynamic sideslip angle with mixed kinematic for accurate control of fast off-road mobile robots. With respect to pure kinematic approaches, the use of this dynamic representation for estimation of the sideslip angle improves reactivity in sliding variable adaptation and consequently in path tracking accuracy.

The content of this paper is mostly based on the publication in [4] on handling model of advanced vehicle dynamics where mathematical algorithms for a single-track vehicle are modelled regarding the effects of the vehicle centre of gravity, the front/rear tire stiffness and the under-steering/over-steering conditions. Other knowledge for yaw damping and steering control is referred in [5] where a steering control system is studied with yaw damping rate and yaw natural frequency to control the unexpected yaw motions. Latest update references are referred to [6-11].

The outline of this paper is as follows: Section 2 provides fundamental mathematic formulas for calculation of vehicle sideslip, section 3 presents the vehicle behaviour with steering in steady state condition, section 4 demonstrates the vehicle movement in transient responses and section 5 analyses the vehicle dynamic responses with frequency input. Finally, conclusion is withdrawn in section 6.

2. VEHICLE SLIDESLIP CALCULATION

When the vehicle is moving straight on a flat surface, the direction of the center of gravity (CG) keeps the same with the orientation of the vehicle. When the vehicle turns, the yaw rate causes the change of the orientation. The vehicle demonstrates a velocity component perpendicular to the orientation, known as the lateral velocity. Then, the orientation of the vehicle and the direction of the travel are no longer the same. The vehicle is moving under the influence of different forces. If a lateral force is acting on the tire, an angle is formed between the direction of movement of the tire and the tire straight line. This angle is called the sideslip angle, see Figure 1.

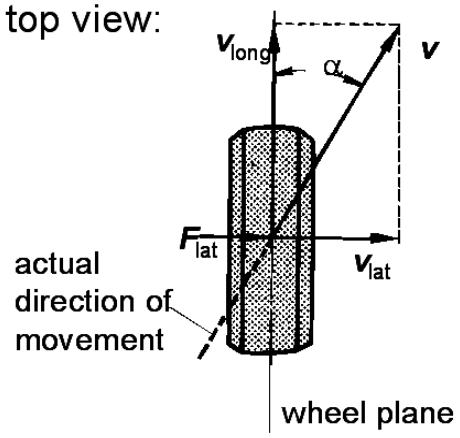

Figure 1. Sideslip angle α.

Reason for this sideslip angle or the tire slip is the elastic lateral deflection of the rolling tire in the tire contact area under the effect of the lateral force between tire and road. For analyzing the motion behaviors of a single-track model, a linearization of the tire lateral force and the tire slip angle is assumed via a tire stiffness c_α, see equation (1):

$$c_\alpha = \frac{F_\alpha}{\alpha} \tag{1}$$

When the vehicle moves at low speed, the wheels roll without a tire slip angle since the lateral cornering force, F_α, is small and can be ignored. The vehicle model can be

seen as the assumption of Rudolf Ackermann with the elongations of all wheel centre lines intersecting at one point, the centre of the turning curve as can be seen in Figure 2.

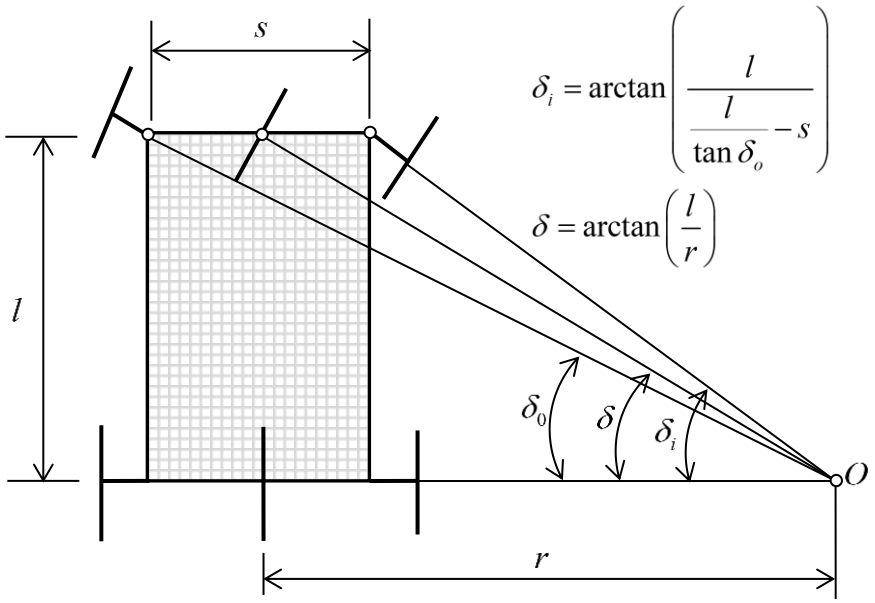

Figure 2. Model for sideslip free at slow speed cornering (Ackermann condition)

where, δ_i, δ_o: steering angle of inner and outer wheel, l: wheel base, s: kingpin track width, r: radius of the curve.

The steering angle, δ, can be simply calculated as equation (2):

$$\delta = \arctan\left(\frac{l}{r}\right) \tag{2}$$

The steering angle of the inner wheel, δ_i, is a function of the steering angle of the outer wheel, δ_o, see equation (3):

$$\delta_i = \arctan\left(\frac{l}{\frac{l}{\tan\delta_o} - s}\right) \tag{3}$$

Furthermore, as a result of Ackermann condition, the angle of the inner wheel, δ_i, is greater than the steering angle at the outer wheel, δ_o.

However, when the lateral force appears, the vehicle front wheel orientation and the vehicle movement direction is no longer the same. A simplified description of the vehicle lateral dynamics is demonstrated in a single-track model, see Figure 3. The tire contact points are in the center of tires. Longitudinal forces in the tire contact points as well as wheel load fluctuations are not considered. The height of the center of gravity is zero

The Newton's law equation of the motion for the vehicle lateral direction is shown in equation (4):

$$ma_y = F_{Lf} + F_{Lr} \tag{4}$$

The force of inertia acting on the vehicle center of gravity, ma_y, corresponds to the centrifugal force, see equation (5):

$$ma_y = m\frac{v^2}{r} = m\frac{v}{r}\dot{v}r = mv(\dot{\Psi} - \dot{\beta}) \tag{5}$$

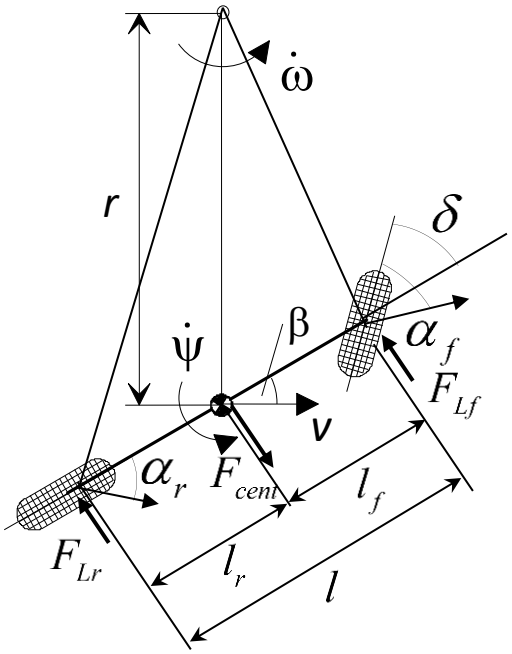

Figure 3. Deflection of the rolling tire by a lateral cornering force F_α.

where, v: vehicle velocity, ω: vehicle angular velocity, r: radius of curve, Ψ: yaw angle, β: side slip angle, δ: steering angle, α: tire slip angle, l: wheel base.

The gyroscopic effect on the z-axis at the vehicle center of gravity has been calculated by equation (6):

$$J\ddot{\Psi} = F_{Lf}l_f - F_{Lr}l_r \tag{6}$$

where J is the vehicle moment of inertia on *z*-axis.

The tire side forces can be calculated from the given tire slip rigidity, c_α, in equation (1) for the front wheel and expressed in equation (7):

$$F_{Lf} = c_{\alpha f}\alpha_f \tag{7}$$

and for the rear wheel, see equation (8):

$$F_{Lr} = c_{\alpha r}\alpha_r \tag{8}$$

The side slip angle for the vehicle at the center of gravity, β, can be formulated from the front tire slip, α_f, see equation (9):

$$\alpha_f = \delta + \beta - \frac{l_f \dot{\Psi}}{v} \tag{9}$$

and from the rear tire slip, α_r, see equation (10):

$$\alpha_r = \beta + \frac{l_r \dot{\Psi}}{v} \tag{10}$$

It is noted that the tire slip rigidity or the sideslip stiffness, c_α, is an elastic property for each rubber tires, normally in the range of 30,000-50,000 N/rad.

3. STEERING IN STEADY STATE

In steady state condition, the vehicle speed, v, is a constant, then, the yaw velocity, $\dot{\Psi}$, and the sideslip, β, are also constant, i.e, $\ddot{\Psi} = 0$ and $\dot{\beta} = 0$.

The torque balance equations can be formulated at the rear contact point, see equation (11):

$$F_{Lf} l = m a_y l_r \tag{11}$$

and at the front contact point it has been expressed by equation (12):

$$F_{Lr} l = m a_y l_f \tag{12}$$

Replaced with the tire slip rigidity in equation (7), it has been expressed equation (13):

$$c_{\alpha f}\left(\delta + \beta - \frac{l_f \dot{\Psi}}{v}\right) = \frac{l_r}{l} m a_y \tag{13}$$

and in equation (8) we will have equation (14):

$$c_{\alpha r}\left(\beta + \frac{l_r \dot{\Psi}}{v}\right) = \frac{l_f}{l} m a_y \tag{14}$$

Due it's the steady state, $\dot{\beta} = 0$, then from equation (5), $\dot{\Psi} = \frac{v}{r}$. The transformation from equation (13) and (14) leads to equation (15):

$$\delta = \frac{l}{r} + \frac{m}{l}\left(\frac{l_r}{c_{\alpha f}} - \frac{l_f}{c_{\alpha r}}\right) a_y \tag{15}$$

From the above equation, the necessary steering angle, δ, during the steady state driving along a curve composes of two parts. The first part, $\frac{l}{r}$, or Ackermann angle, depends on the vehicle geometrical parameters. And the second part, $\frac{m}{l}\left(\frac{l_r}{c_{\alpha f}} - \frac{l_f}{c_{\alpha r}}\right) a_y$,

is characterized by the influences of the lateral acceleration and the tire rigidities, which can increase, if $\left(\frac{l_r}{c_{\alpha f}} > \frac{l_f}{c_{\alpha r}}\right)$, or reduce, if $\left(\frac{l_r}{c_{\alpha f}} < \frac{l_f}{c_{\alpha r}}\right)$, the steering angle.

From equation (9) and (10), the sideslip angle difference between the front and the rear wheel is expressed by equation (16):

$$\Delta\alpha = \alpha_f - \alpha_r = \delta - \frac{l\dot{\Psi}}{v} \tag{16}$$

With $v = \dot{\Psi} r$, then, $\Delta\alpha = \delta - \frac{l}{r}$. Replace with δ in equation (15) we will have equation (17):

$$\Delta\alpha = \frac{m}{l}\left(\frac{l_f}{c_{\alpha r}} - \frac{l_r}{c_{\alpha f}}\right) a_y \tag{17}$$

Then, the difference of the sideslip angles depends on the vehicle and the tire parameters. The driver has to compensate the sideslip angle difference, $\Delta\alpha$, with the steering angle, δ. This forms a basic knowledge of over-steer and under-steer definition: Over-steer is if $\Delta\alpha = \alpha_f - \alpha_r < 0$, neutral is if $\Delta\alpha = \alpha_f - \alpha_r = 0$, and under-steer is if $\Delta\alpha = \alpha_f - \alpha_r > 0$, see Figure 4.

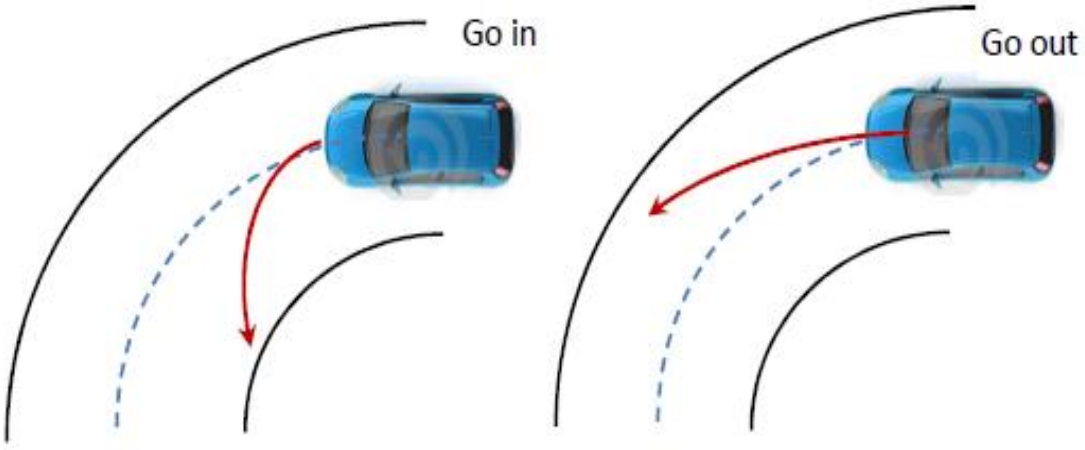

Figure 4. Over-steer (left) and Under-steer (right).

Under-steer and over-steer are vehicle dynamic characteristics used to demonstrate the sensitivity of a vehicle steering system. The under-steer happens if the vehicle turns less than the steering control of the driver. Conversely, over-steer happens if the vehicle turns more than the steering control of the driver.

The under-steer system is safer since it causes the reduction of the lateral force at the rear axle and makes the vehicle to stabilize at a smaller curve radius with less lateral acceleration. While the over-steer vehicle is more dangerous because it increases the lateral force and increases the swerve tendency of the vehicle.

Figure 5 depicts the relationship between the sideslip and steering angle with the vehicle speed and the turning radius. When maintaining the turning radius at $r = 100m$

and varying the vehicle speeds, $0 \le v \le 40m/s$, the sideslips increase exponentially and steering angles rise, $1.4^0 \le \delta \le 3.2^0$.

Similarly, when reducing the turning radius $100 \le r \le 10m$, the sideslips increase exponentially and steering angles rise $2^0 \le \delta \le 20^0$.

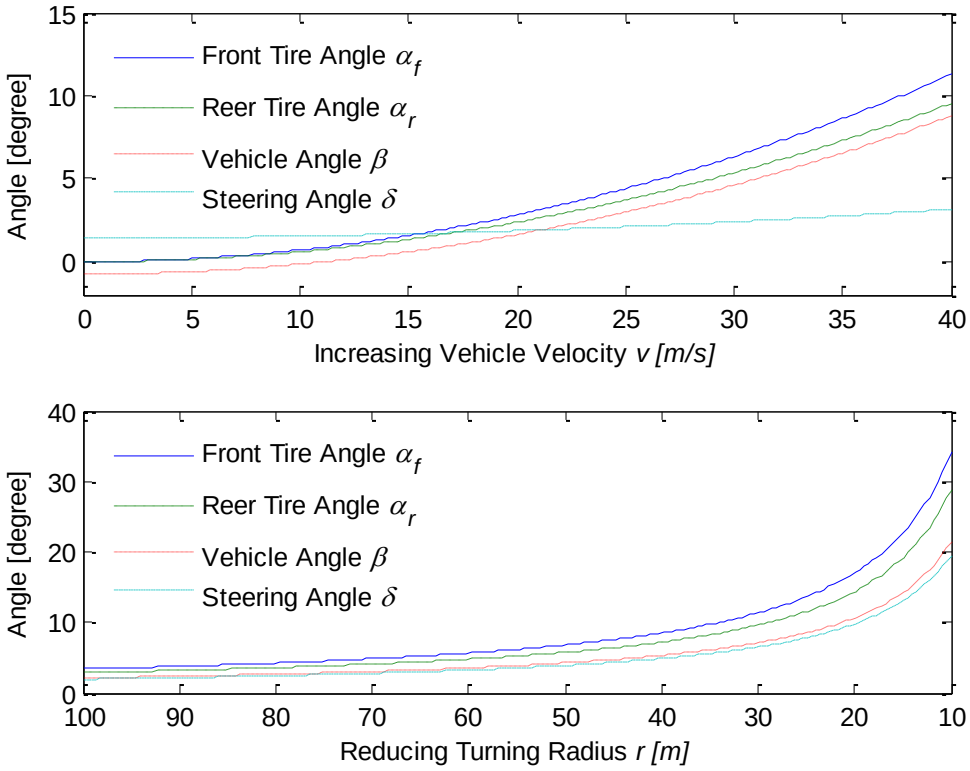

Figure 5. Side and steering angle vs. velocity and turning radius

4. STEERING MOVEMENT IN TRANSIENT RESPONSE

Transformation of equations (4-10) can lead to the following expressions:

$$mv(\dot{\psi} - \dot{\beta}) = c_{\alpha f}\left(\delta + \beta - \frac{l_f}{v}\dot{\psi}\right) + c_{\alpha r}\left(\beta + \frac{l_r}{v}\dot{\psi}\right) \tag{18}$$

and

$$J_Z\ddot{\psi} = c_{\alpha f}\left(\delta + \beta - \frac{l_f}{v}\dot{\psi}\right)l_f - c_{\alpha r}\left(\beta + \frac{l_r}{v}\dot{\psi}\right)l_r \tag{19}$$

Equation (18) can be represented by yaw velocity, $\dot{\psi}$, see equations (20-21):

$$\dot{\psi} = \frac{mv\dot{\beta} + c_{\alpha f}(\delta + \beta) + c_{\alpha r}\beta}{mv - c_{\alpha r}\frac{l_f}{v} + c_{\alpha f}\frac{l_r}{v}} \tag{20}$$

For the steady state, $v = const$, then, $\ddot{\psi}$:

$$\ddot{\psi} = \frac{mv\ddot{\beta} + c_{\alpha f}(\dot{\delta} + \dot{\beta}) + c_{\alpha r}\dot{\beta}}{mv - c_{\alpha r}\frac{l_r}{v} + c_{\alpha f}\frac{l_f}{v}} \tag{21}$$

Replace $\dot{\psi}$ and $\ddot{\psi}$ in equation (19) and we will have the equation (22):

$$\begin{aligned} &\ddot{\beta} + \left(\frac{c_{\alpha f} + c_{\alpha r}}{mv} + \frac{c_{\alpha f} l_f{}^2 + c_{\alpha r} l_r{}^2}{vJ_Z}\right)\dot{\beta} \\ &+ \left(\frac{c_{\alpha r} l_r - c_{\alpha f} l_f}{J_Z} + \frac{c_{\alpha f} c_{\alpha r} l^2}{J_Z mv^2}\right)\beta \\ &= \left(\frac{c_{\alpha f} l_f}{J_Z} - \frac{c_{\alpha f} c_{\alpha r}(l_f l_r + l_r{}^2)}{J_Z mv^2}\right)\delta - \frac{c_{\alpha f}}{mv}\dot{\delta} \end{aligned} \tag{22}$$

The characteristic polynomial of the dynamic equation in (22) can be represented in an inhomogeneous linear differential equation of 2nd order for the vehicle slip angle β. The homogeneous part of this differential equation has the form of a simple oscillating motion with damping:

$$\ddot{\beta} + A\dot{\beta} + B\beta = 0 \tag{23}$$

or in the vibrated frequency form:

$$\omega_0^2 + 2D\omega_0 s + s^2 = 0 \tag{24}$$

Thus, the differential equation for the slip angle β can be viewed with a yaw undamped natural frequency, ω_0:

$$\omega_0 = \sqrt{\frac{c_{\alpha r} l_r - c_{\alpha f} l_f}{J_Z} + \frac{c_{\alpha f} c_{\alpha r} l^2}{J_Z mv^2}} \tag{25}$$

and with a yaw damping rate D:

$$D = \frac{\frac{c_{\alpha f} + c_{\alpha r}}{mv} + \frac{c_{\alpha f} l_f{}^2 + c_{\alpha r} l_r{}^2}{J_Z v}}{2\omega_0} \tag{26}$$

Then, the dynamic yaw frequency, ω_{omD}, is:

$$\omega_{0mD} = \sqrt{1 - D^2}\,\omega_0 \tag{27}$$

The yaw natural frequency and damping rate can be represented for the movement of the vehicle around the vertical axis (z).

5. VEHICLE DYNAMIC ANALYSIS

The linearized single-track vehicle model is now examined under the reaction of the driver to control the vehicle movement with the input variable, the steering angle, δ. The output variables are the yaw velocity, $\dot{\psi}$, and the lateral acceleration, a_y.

The transfer function of the output, $\dot{\psi}$, and the input, δ can be derived from equation (14) with $\frac{1}{r} = \frac{\dot{\psi}}{v}$ and $a_y = v\dot{\psi}$, then:

$$\left(\frac{\dot{\psi}}{\delta}\right)_{stat} = \frac{v}{l + \frac{m}{l}\left(\frac{l_r}{c_{sf}} - \frac{l_f}{c_{sr}}\right)v^2} \tag{28}$$

where the relation $\left(\frac{\dot{\psi}}{\delta}\right)_{stat}$ is referred to as the stationary yaw amplification factor.

For analyzing the dynamic behavior of the vehicle, equations (18) and (19) can be converted to Laplace *s*-form as shown in equation (29):

$$\frac{\dot{\psi}}{\delta} = F(s) = \left(\frac{\dot{\psi}}{\delta}\right)_{stat} \frac{1 + T_z s}{1 + \frac{2D}{\omega_0}s + \frac{1}{\omega_0^2}s^2} \tag{29}$$

with T_z is a time constant, $T_z = \frac{mvl_f}{c_{\alpha r} l}$.

This Laplace *s*-form can also be transformed for the lateral acceleration, see equation (30):

$$\frac{a_y}{\delta} = F'(s) = \left(\frac{a_y}{\delta}\right)_{stat} \frac{1 + T_1 s + T_2 s^2}{1 + \frac{2D}{\omega_0}s + \frac{1}{\omega_0^2}s^2} \tag{30}$$

with the time constant $T_1 = \frac{l_r}{v}$, and $T_2 = \frac{J_Z}{c_{\alpha r} l}$.

Simulations for the driving control of the vehicle movement are conducted with a step steering (sudden step in input signal) and shown in Figure 6.

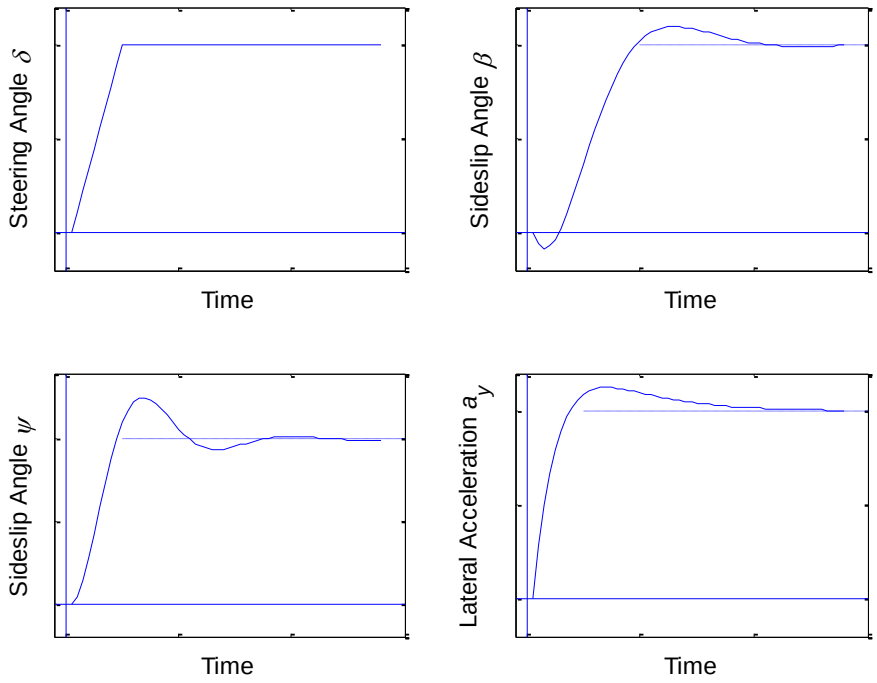

Figure 6. Transient response with a steering step angle

For a very fast input of a steering step angle to 20^0 in 0.4 second, the sideslip angle, ψ , and the lateral acceleration, a_y, respond with a small overshooting motion and then steadily fluctuate at the stable position; While the sideslip angle, β, responds in an undershooting motion at the beginning time.

For frequency response, the transfer function in equation (29) now is transformed into the frequency, $j\omega$, form at equation (31):

$$F(j\omega) = \left(\frac{\dot{\psi}}{\delta}\right)_{stat.} \frac{1+T_z j\omega}{1+\frac{2\cdot D}{\omega_0} j\omega - \frac{\omega^2}{\omega_0^2}} \tag{31}$$

The amplitude, $\left(\frac{\hat{\dot{\psi}}}{\hat{\delta}}\right) = |F(j\omega)|$, is thus a frequency dependence.

The lateral acceleration in equation (30) is now applied for the frequency response at equation (32):

$$F'(j\omega) = \left(\frac{a_y}{\delta}\right)_{stat.} \frac{1+T_1 j\omega - T_2\cdot\omega^2}{1+\frac{2\cdot D}{\omega_0} j\omega - \frac{\omega^2}{\omega_0^2}} \tag{32}$$

Simulation results of frequency response are shown in figure 7. There is a peak of magnitude and phase shifting in the low frequencies. The amplitude responses drop in high frequencies. There is a phase lag in yaw velocity and thus, the vehicle reaction on the steering angle becomes larger in low frequencies.

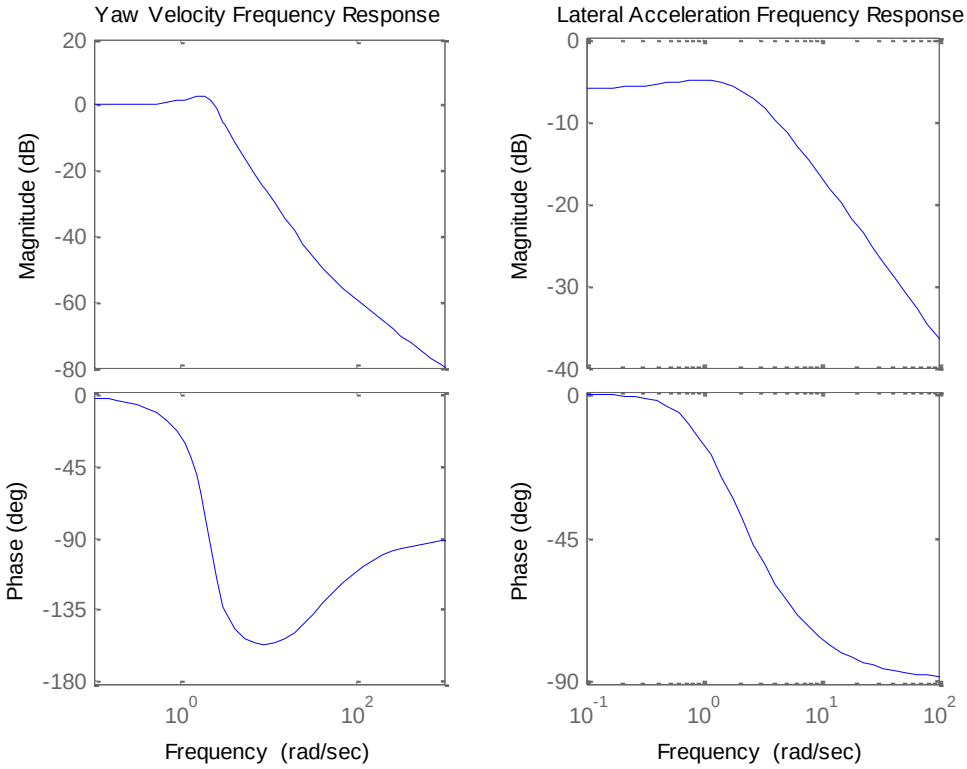

Figure 7. Frequency response with yaw velocity and lateral acceleration

6. CONCLUSION

The single-track vehicle model allows analyzing the influences of fundamental parameters such as the effect of the location of the center of gravity, the different front and rear cornering stiffness as well as the under-steering/over-steering systems on the vehicle dynamic behavior and sideslip angle. Results from this study can be applied to estimate the tracking errors for an automatic vehicle tracking system in the next step of the project. The analysis of the transient response for this system provides essential knowledge of the vehicle dynamic behaviors under the influences of nonlinear dynamic variables.

CONFLICT OF INTERESTS

The authors would like to confirm that there is no conflict of interests associated with this publication and there is no financial fund for this work that can affect the research outcomes.

REFERENCES

[1] Kim H. and Ryu J. Sideslip Angle Estimation Considering Short-duration Longitudinal Velocity Variation, *International Journal of Automotive Technology*, 2011; 12(4); 545-553.

[2] Hac A., Nichols D. and Sygnarowicz D. Estimation of Vehicle Roll Angle and Side Slip for Crash Sensing, *SAE International Congress*, 2010; 1; 1-11.

[3] Lenain R., Thuilot B., Cariou Ch. and Martinet P. Mixed Kinematic and Dynamic sideslip angle Observer for accurate Control of Fast Off-road Mobile Robots, *Journal of Field Robotics*, 2010; 27(2); 181-196.

[4] Minh V.T. *Advanced Vehicle Dynamics*, 1st edition, Malaya Press, Pantai Valley, 50603. Kuala Lumpur, Malaysia.

[5] Ackermann J. and Sienel W. Robust Yaw Damping of Cars with Front and Rear Wheel Steering", *IEEE Transactions on Control Systems Technology*, 1993; 1(1); 15-20.

[6] Minh V.T., Moezzi R., Cyrus J. and Dhoska K. Smart Mechatronic Elbow Brace using EMG Sensors. *International Journal of Innovative Technology and Interdisciplinary Sciences*, 2022; 5(2); 865-873.

[7] Minh V.T., Katushin N., Moezzi R., Dhoska K. and Pumwa J. Smart Glove for Augmented and Virtual Reality. *International Journal of Innovative Technology and Interdisciplinary Sciences*, 2021; 4(2); 663-671.

[8] Minh V.T., Moezzi R., Dhoska K. and Pumwa J. Model Predictive Control for Autonomous Vehicle Tracking. *International Journal of Innovative Technology and Interdisciplinary Sciences*, 2021; 4(1); 560-603.

[9] Minh V.T., Tamre M., Musalimov V., Kovalenko P., Rubinshtein I., Ovchinnikov, I. and Moezzi R. Simulation of Human Gait Movements. *International Journal of Innovative Technology and Interdisciplinary Sciences*, 2020; 3(1); 326-345.

[10] Minh V.T. Conditions for stabilizability of linear switched systems, *AIP Conference Proceedings*, 2011; 1337(1); 108-112.

[11] Minh V.T. and Hashim F.B.M. Tracking setpoint robust model predictive control for input saturated and softened state constraints, *International Journal of Control, Automation and Systems*, 2011; 9(5), 958-965.